Microscopic calculation of spin waves in antiferromagnetically coupled multilayers: Nonreciprocity and finite-size effects

F. C. Nörtemann,* R. L. Stamps, and R. E. Camley
Department of Physics, University of Colorado at Colorado Springs, Colorado Springs, Colorado 80933-7150
(Received 30 November 1992)

We present a calculation of spin waves in coupled multilayered structures that is based on exact evaluation of both exchange and dipolar fields. We compare our results with earlier continuum treatments. The gound-state spin configuration in antiferromagnetically coupled multilayers can differ significantly from the uniformly canted ground state usually assumed. This nonuniform ground state is found to alter radically the character of the spin-wave modes and sometimes lead to a strong localization of the wave to the outermost magnetic films of the multilayer. In addition, we examine the validity of effective-medium theory—a continuum theory—and find that it does not completely describe spin-wave excitations in finite antiferromagnetically coupled multilayers. Finally, the spin-wave frequencies are found to be nonreciprocal with respect to propagation direction for most directions, i.e., $\omega(\mathbf{q})\neq\omega(-\mathbf{q})$ where $\mathbf{q}$ is the propagation wave vector. This nonreciprocal behavior is explained from basic symmetry considerations. Again, the nonreciprocity is not properly described within effective-medium theory.

I. INTRODUCTION

The discovery of antiferromagnetic coupling between ferromagnetic films across nonmagnetic layers[1] has raised several important questions and resulted in a number of exciting potential applications. For example, one of the most fascinating phenomena associated with antiferromagnetic coupling is the giant magnetoresistance effect.[2–4] It has been found that a system of antiparallel ferromagnetic films has upward to a 60% higher electrical resistance than parallel ferromagnetic films. Even though the actual spin configuration may play a very important role in such phenomena, to date theoretical investigations[5–7] of giant magnetoresistance and dynamic response of antiferromagnetically coupled systems have assumed only the simplest possible magnetic ground states.

In a recent paper,[8] we showed that multilayered systems of antiferromagnetically coupled films will have complicated ground states that are strongly field dependent. Some of these ground states are quite different from the ground state assumed by previous theoretical studies of these systems. In the present work we discuss the effects of the correct ground state on the linear dynamic magnetic behavior of multilayer systems. Spin-wave excitations in these systems are interesting for several reasons. One reason is that the experimental study of spin-wave excitations has proven invaluable in the past in characterizing the properties of many different types of magnetic structures.[9,10] A second reason is that there have previously been no realistic theoretical models for long-wavelength spin-wave excitations in noncollinear antiferromagnetically coupled multilayers outside of attempts which made use of effective-medium theory.[11–14]

Effective-medium theory is a very elegant method of calculating long-wavelength excitations in superlattices. The essence of the theory is to assume that the wavelength of the excitation is long in comparison to the size of a unit cell so that the amplitude of the wave is approximately constant across the unit cell. This allows for several simplifying assumptions that make it possible to perform calculations of dynamics for what are otherwise hopelessly complicated superlattice structures.

In this paper we present a microscopic calculation of spin-wave frequencies in magnetic multilayer structures which makes no restrictions on the allowed ground-state magnetic configurations and which does not make the drastic assumptions of effective-medium theory. We will use this model to discuss the effects of complicated ground states on spin-wave frequencies and characteristics. We also examine the validity of effective-medium models for these systems by direct comparison to our microscopic model. As expected effective medium cannot describe short-wavelength excitations. Furthermore, we will see that in some cases it does not properly predict the behavior of long-wavelength spin-wave excitations in *finite* antiferromagnetically coupled systems.

We now review the important features of the ground-state configurations before presenting our spin-wave calculations. The geometry of the multilayer is shown in Fig. 1. The axis of the multilayer lies along the y direction, an external applied magnetic field H_0 is directed along the z axis, and the magnetizations in each layer lie in the xz plane some angle α from the z axis. The magnetic layers are identified by the integer n and the angle α_n for the magnetization of each layer by the subscript n. The number of atomic layers in each magnetic film is N and there are a total of L magnetic layers in the multilayer. The number of atomic layers in each nonmagnetic film is N_s. For simplicity we assume that the lattice is simple cubic with spacing a. The thicknesses of the magnetic films are then Na and the thicknesses of the nonmagnetic layers are $N_s a$. For future reference, we also define a wave vector $\mathbf{q}$ that lies in the xz plane at an angle

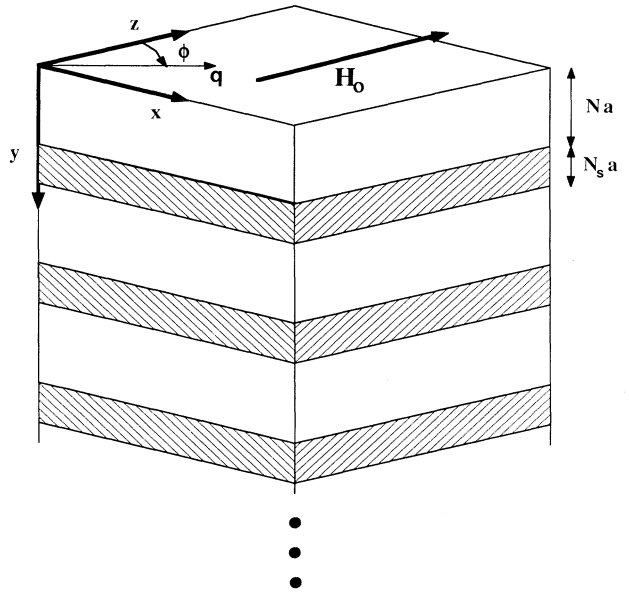

FIG. 1. Geometry. The axis of the multilayer is in the y direction and an external magnetic field is applied in the z direction. A wave vector $\mathbf{q}$ is defined in the xz plane that makes an angle ϕ with the z axis. The magnetic films consist of N atomic layers with a lattice spacing of a. There are N_s nonmagnetic layers between each magnetic film. There are L magnetic films in the multilayer.

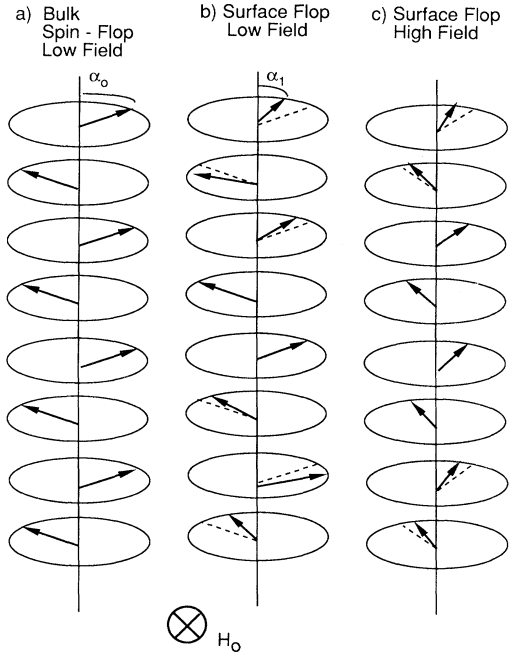

FIG. 2. Spin configurations. Each arrow represents the magnetization of a magnetic film. The uniform ground state is shown in (a) where the magnetization of each film is canted in the xz plane an angle α away from the field direction. The dotted lines in (b) and (c) are the α given by Eq. (1) for a uniform state. A low-field configuration for a finite multilayer is shown in (b) and a high-field configuration is shown in (c).

ϕ from the z axis.

If $|\alpha_n|$ were independent of position then the magnetization of each film would be canted away from the applied field direction by an amount α given by

$$\cos\alpha = -g\mu_B LNH_0/4(L-1)J_i S \ . \tag{1}$$

Here J_i is the interlayer exchange energy, g is the g factor, and μ_B is the Bohr magnetron. S is the spin value. Note that the sign convention is such that a negative J_i denotes antiferromagnetic coupling. In the remainder of this paper we refer to this angle α as the "bulk" canting angle. This ground-state configuration is sketched in Fig. 2(a). The arrows represent the net magnetization in each magnetic film. Here the magnetization of each film is canted away from the direction of the field by the angle α calculated according to Eq. (1).

A canted state where every canting angle is given by Eq. (1) is not stable for a finite multilayer. The reason is that in a finite multilayer the outermost films experience only half the interlayer exchange coupling compared to a film inside the multilayer. Because of competition between antiferromagnetic exchange and Zeeman energies, it is energetically favorable to rotate the outermost magnetizations away from the bulk angle given by Eq. (1) in such a way as to lower the net Zeeman energy for the entire structure.

The lowest-energy stable states are somewhat complicated and strongly dependent on the magnitude of the external applied field.[8] These states are depicted in Fig. 2(b) for small field strengths and in Fig. 2(c) for larger field strengths. The dotted lines are the bulk α given by Eq. (1) for large L. At high fields, the angles α_n of the outermost spins are less than the bulk α. For low fields, the size of the angles alternate with respect to the bulk α from layer to layer. Note that the equilibrium magnetizations all lie in the field direction for fields greater than $4J_i S/g\mu_B$.

The largest angular deviations from the bulk value occurs for magnetizations in the outermost layers. We might expect that any modes of the system which are localized to the outermost layers will be the most strongly affected by the nonuniform canting. We will see that this is indeed the case.

In the next section we present a theory for magnetostatic spin waves in multilayers which includes both dipolar and exchange interactions. In Sec. III, we examine the general features of the allowed spin-wave modes and compare the results of this microscopic theory to those obtained using an effective-medium approach. In Sec. IV, we study the allowed spin-wave excitations for ground states similar to those shown in Figs. 2(b) and 2(c). In Sec. V, we discuss the effects of canting and out-of-plane anisotropy on the stability of the equilibrium spin configuration. Finally, in Sec. VI, we discuss the dependence of spin-wave energies on propagation direction and show that the spin-wave energies can differ de-

pending on whether the wave is traveling forward or backward for most propagation directions. We refer to this behavior as nonreciprocity where $\omega(\mathbf{q})\neq\omega(-\mathbf{q})$.

II. THEORY

The geometry is the same as that of Fig. 1. As in the above discussion, all layer-dependent variables are indexed by the integer n. The spins are treated as point dipoles arranged in a cubic lattice structure within each film. A Heisenberg exchange interaction is assumed of the form

$$H_{\rm ex}=\frac{1}{2}\sum_{\mathbf{r},\mathbf{r}'}{}' J(\mathbf{r}-\mathbf{r}')\mathbf{S}(\mathbf{r})\cdot\mathbf{S}(\mathbf{r}') \ . \tag{2}$$

The notation is as follows: $\mathbf{S}(\mathbf{r})$ is the spin operator at lattice site $\mathbf{r}$ and J is the exchange constant written as a function of the distance between lattice sites. The sum is taken over all magnetic lattice sites in the multilayer and the prime on the sum means that the terms $\mathbf{r}=\mathbf{r}'$ are excluded. In what follows we assume exchange coupling between nearest neighbors only with exchange constant J. We assume a coupling constant J_i between spins on the outermost layers of adjacent films.

The spins are also coupled via dipolar interactions:

$$H_{\rm dip}=(g\mu_B)^2\sum_{\mathbf{r},\mathbf{r}'}{}'\left[\frac{\mathbf{S}(\mathbf{r})\cdot\mathbf{S}(\mathbf{r}')}{|\mathbf{r}-\mathbf{r}'|^3}-3\frac{[\mathbf{r}\cdot\mathbf{S}(\mathbf{r})][\mathbf{r}'\cdot\mathbf{S}(\mathbf{r}')]}{|\mathbf{r}-\mathbf{r}'|^5}\right] . \tag{3}$$

This interaction is long ranged and the sum includes all spins in the multilayer system.

The complete Hamiltonian including a Zeeman energy term due to an external magnetic field H_0 is

$$H=H_{\rm ex}+H_{\rm dip}-g\mu_B\sum_{\mathbf{r}'}\mathbf{H}_0\cdot\mathbf{S}(\mathbf{r}') \ . \tag{4}$$

Next, equations of motions are constructed using the appropriate commutation rules for the spin operators. We then consider the long-wavelength region where the spin operators can be treated as classical vectors.

We are interested in small-amplitude excitations so we want to first linearize the equations of motion. This is accomplished by separating the spin variables into a static part $\mathbf{S}(\mathbf{r})$, and a dynamic part $\mathbf{s}(\mathbf{r},t)$:

$$\mathbf{S}(\mathbf{r},t)\rightarrow\mathbf{s}(\mathbf{r},t)+\mathbf{S}(\mathbf{r}) \ . \tag{5}$$

Terms of second order in $\mathbf{s}(\mathbf{r},t)$ are then neglected in the equations of motion. Finally, we assume translational invariance in the xz plane. We thus choose plane-wave solutions for $\mathbf{s}(\mathbf{r},t)$ of the form

$$\mathbf{s}(\mathbf{r},t)=\mathbf{s}_n e^{i(q\cdot r_{\parallel}-\omega t)} \ . \tag{6}$$

Note that the position in the y direction is now given by the subscript n. The position in the xz plane is given by $\mathbf{r}_{\parallel}$. Furthermore, we may then write

$$\mathbf{S}(\mathbf{r})=\mathbf{S}_n \tag{7}$$

since the static part is independent of position in the xz plane but may vary from one layer to another.

The resultant linearized equations of motion for spins within a film are

$$\begin{aligned}-i\hbar\omega\mathbf{s}_n=&\mathbf{s}_n\times[g\mu_B(\hat{\mathbf{z}}H_0+\mathbf{H}_n^s)+4J\mathbf{S}_n+J_{n,n-1}\mathbf{S}_{n-1}+J_{n,n+1}\mathbf{S}_{n+1}]\\&+\mathbf{S}_n\times[g\mu_B\mathbf{h}_n(\mathbf{q})+2J\mathbf{s}_n(\cos q_x a+\cos q_z a)+J_{n,n-1}\mathbf{s}_{n-1}+J_{n,n+1}\mathbf{s}_{n+1}] \ .\end{aligned} \tag{8}$$

Here a is the lattice spacing within a film. The exchange constant $J_{n,m}$ is defined as $J_{n,m}=J$ when n and m are in the same magnetic film; $J_{n,m}=J_i$ when n and m are the outermost layers of neighboring magnetic films; and $J_{n,m}=0$ when n or m is an outermost layer of the multilayer. The dipolar terms are contained in $\mathbf{H}^s$ and $\mathbf{h}(\mathbf{q})$. Fields which are independent of $\mathbf{q}$ are written in $\mathbf{H}^s$ and $\mathbf{q}$-dependent dipolar fields are written in $\mathbf{h}(\mathbf{q})$. Both of these fields can be put in terms of the components of a tensor $\mathbf{g}(\mathbf{q};n-n')$ as follows:

$$\mathbf{h}_n(\mathbf{q})=g\mu_B\sum_{n'}\overleftrightarrow{g}(\mathbf{q};n-n')\mathbf{s}_{n'} \ , \tag{9}$$

$$\mathbf{H}_n^s=g\mu_B\sum_{n'}\overleftrightarrow{g}(0;n-n')\mathbf{S}_{n'} \ . \tag{10}$$

The tensor $\overleftrightarrow{g}$ describes the $\mathbf{q}$-dependent coupling between the spins in layer n and the spins in layer n'. Forms for $\overleftrightarrow{g}$ are discussed later and given in the Appendix.

The complete set of coupled equations of motion define a large but straightforward eigenvalue problem. The equations of motion can be put in form

$$[\overleftrightarrow{M}-\omega]\begin{bmatrix}\mathbf{s}_1\\ \mathbf{s}_2\\ \vdots\end{bmatrix}=0 \ . \tag{11}$$

The matrix $\overleftrightarrow{M}$ contains the information from the right-hand side of Eq. (8). The particular choice of ground state enters in the direction of the $\mathbf{S}_n$. These are defined in terms of the angle α_n as

$$\mathbf{S}_n=\hat{\mathbf{x}}S\sin\alpha_n+\hat{\mathbf{z}}S\cos\alpha_n \ . \tag{12}$$

The calculational procedure is as follows: Low temperatures are assumed and the ground state is found using a numerical mean-field approach which gives the angles α_n. The ground-state calculation is explained in detail in Ref. 8. Next the eigenvalue problem is solved for the eigenfrequencies ω and eigenvectors. We note that the matrix M is not Hermitian, so care must be taken in finding the correct set of right and left eigenvectors. The right eigenvectors satisfy Eq. (11) and the left eigenvectors satisfy

$$[\mathbf{s}_1\mathbf{s}_2\cdots][\vec{M}-\omega]=0\ . \tag{13}$$

We will refer to right and left eigenvectors as $\mathbf{s}_r$ and $\mathbf{s}_l$.

We also note that when dealing with large numbers of layers, it is helpful to write the equation of motion matrix in a slightly different way. The reason is that, in the coordinate system defined in Fig. 1, there will be three equations of motion for each layer of spins. The order of the matrix M is thus three times the total number of magnetic layers. This number can be reduced by writing the equations of motion in different coordinate systems. This is because there are only two equations of motion for $\mathbf{s}_n$ in a coordinate system rotated an angle α_n from the direction of the field. This rotation puts the z axis of the local frame along the direction of the static magnetization $\mathbf{S}_n$. The total number of equations can thus be reduced by one-third by writing the equations of motion for each $\mathbf{s}_n$ in their own coordinate systems.

We now pause to discuss the treatment of the dipolar terms in Eqs. (9) and (10). The lattice sums in Eq. (3) converge very slowly, especially for small q. Fortunately techniques exist which allow these sums to be put in rapidly convergent forms. These procedures are described in Ref. 15 and the results for our problem are given in the Appendix. The exact forms given in the Appendix are not necessary under all circumstances, however. The first terms of Eqs. (A1)–(A6) dominate for small q when $\mathbf{S}_n$ from different layers are parallel. This is because the magnitude of the remaining terms fall off as $\exp[-qa(k^2+m^2)^{1/2}]$, where m and k are integers greater than 0. The physical interpretation is that the q-dependent $k,m\neq 0$ terms describe the discrete nature of the spin lattice while the $k,m=0$ terms are the continuum limit form of the dipolar fields. The q-dependent $k,m=0$ terms can, in fact, be derived from the magnetostatic Maxwell equations for a planar geometry. The form for $\vec{g}(\mathbf{q};n-n')$ under this approximation is

$$\vec{g}(\mathbf{q},n-n')=2\pi qa\begin{bmatrix}\sin^2\varphi & i\,\mathrm{sgn}(n-n')\sin\varphi & \sin\varphi\cos\varphi\\ i\,\mathrm{sgn}(n-n')\sin\varphi & -1 & i\,\mathrm{sgn}(n-n')\cos\varphi\\ \sin\varphi\cos\varphi & i\,\mathrm{sgn}(n-n')\cos\varphi & \cos^2\varphi\end{bmatrix}e^{-qa|n-n'|}\ . \tag{14}$$

The $k,m\neq 0$ terms become important when $\mathbf{S}_n$ from different layers are no longer parallel. Due to the exponential decay of the $k,m\neq 0$ terms, however, these terms will not be significant for small q unless the nonparallel $\mathbf{S}_n$ are very close; i.e., when the spacing between the two nonparallel $\mathbf{S}_n$ is only on the order of one or two lattice constants. For multilayers constructed by alternating ferromagnetic with nonmagnetic layers, the $k,m\neq 0$ terms will usually be negligible for realistic nonmagnetic layer thicknesses.

A suitable approximation can also be made for the $q=0$ terms. A spin in the interior of a film would experience a $q=0$ field ($\mathbf{H}^s$) containing contributions from the sample demagnetizing fields as well as the local Lorentz field. These fields are given by

$$\vec{g}(0,n-n')=4\pi\begin{bmatrix}\frac{2}{3} & 0 & 0\\ 0 & -1 & 0\\ 0 & 0 & \frac{2}{3}\end{bmatrix}\delta_{nn'}\ . \tag{15}$$

This representation does not properly represent the local fields for a spin near an interface, but the error involved is very small.

III. GENERAL FEATURES AND EFFECTIVE-MEDIUM THEORY

The general features of the allowed spin-wave modes are most simply illustrated by first examining spin-wave propagation assuming the uniform ground state defined by Eq. (1). Later, this will allow us to compare our results to those obtained using an effective-medium approach which also assumes a uniform ground state. Unless otherwise specified, we use the following parameters in all the examples presented in this paper. $N/N_s=2$, $L=10$, $J=10$ J cm^2, $J_i=0.001$ J cm^2, $qa=0.001$, and $\phi=90°$. Also, we use $\vec{g}(q;n-n')$ as given in Eq. (14). The results are given in terms of unitless variables Ω and h where

$$\Omega=\frac{\hbar\omega}{4\pi M_s} \tag{16}$$

and

$$h=\frac{g\mu_B H_0}{4J_i}\ . \tag{17}$$

The saturation magnetization M_s is given by $\rho g\mu_B S$, where ρ is the number of spins per unit volume.

As pointed out in the Introduction, the uniform ground state is not stable, and we expect that some spin-wave modes will soften at certain applied field strengths. This can be seen in Fig. 3 where the lowest ten spin-wave frequencies are shown as functions of applied field assuming a uniform canted ground state. We have numbered the modes at $h=0$ in order to simplify future discussions. The modes are numbered beginning with the highest-frequency mode as mode 1 and ending with the lowest-frequency mode as mode 10. The canting angle is given by Eq. (1) and the critical field, h_c, at which the spins align parallel, occurs for $\alpha=0$. For our ten-film system $h_c=0.9$. A mode softens for an h near 0.85 and reappears at $h=1$. This gap where the mode disappears indicates that the uniform ground state is not stable for h values near h_c.

The modes can be characterized through the magnitude of the spin fluctuations in each film of the multilayer. Note that in order to calculate the magnitudes of the

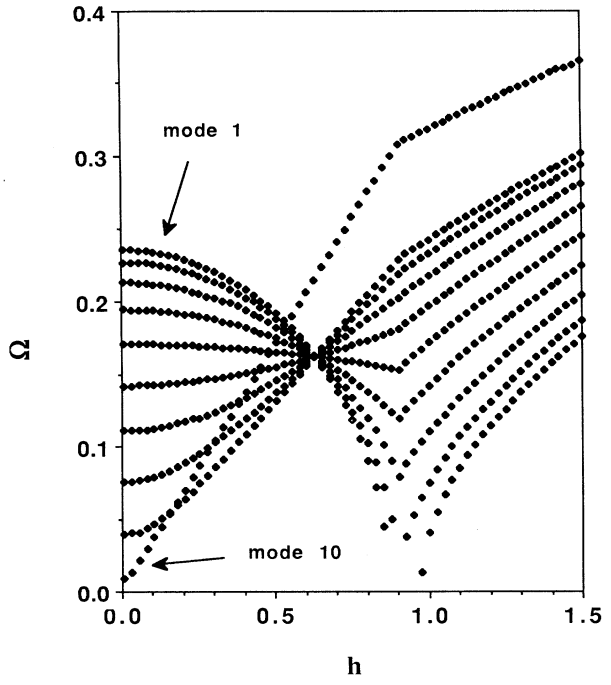

FIG. 3. Frequencies in the uniform canted state. The lowest spin-wave frequencies are shown as functions of applied field for the ten-film multilayer. The canting angle α is given by Eq. (1). The magnetizations are oriented away from the field for $h<1$ and parallel to the field for $h>1$. Propagation is perpendicular to the field direction. The modes are numbered for future reference as shown.

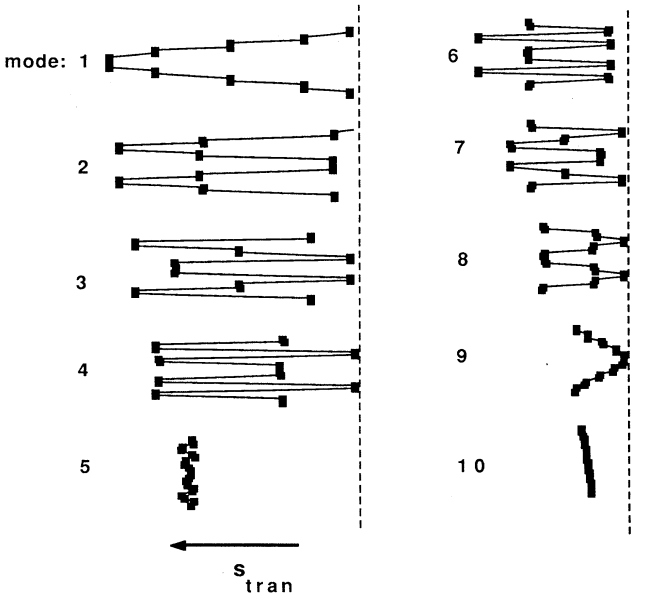

FIG. 4. Mode profiles at $h=0.05$. The transverse magnitudes of spin fluctuations in the yx plane are shown for each of the ten lowest-energy modes from Fig. 3. Note the localization of mode 10 to one side of the multilayer.

spin fluctuations, both the right and left eigenvectors $\mathbf{s}_r$ and $\mathbf{s}_l$ are required, as discussed above. It will be useful to define a transverse magnitude as

$$s_{\text{tran}}=s_{lx}s_{rx}+s_{ly}s_{ry} \tag{18}$$

and a longitudinal magnitude as

$$s_{\text{long}}=s_{lz}s_{rz}\ . \tag{19}$$

In Fig. 4 we show s_{tran} as a function of position in the multilayer for each of the ten modes of Fig. 3 at a small h value of 0.05. The mode profiles are labeled such that profile 1 represents the highest-frequency mode and profile 10 is the lowest-frequency mode. Profile 10 is the Damon-Eshbach mode—the long-wavelength surface mode—of the multilayer stack. Note the slight localization of this mode to the upper outermost film of the multilayer. This mode is thus a surface mode in the transverse fluctuations. We note that a plot of s_{long} appears practically identical to s_{tran} with the exception that s_{long} for mode 10 is uniform across the multilayer and not localized to an outer film.

Some insight can be gained by noting that the unit cell for an infinite superlattice with a uniformly canted ground state consists of two magnetic and two nonmagnetic films. The magnetization of each magnetic film is canted away from the field direction as shown in Fig. 2. There are two possible ways for the magnetizations within a unit cell to precess with respect to one another. These are shown in Figs. 5(a) and 5(b). In Fig. 5(a), the magnetizations precess together in phase, and in Fig. 5(b), the magnetizations precess 180° out of phase with respect to one another. The coupled excitations of the superlattice then form two bands: one band consisting of Bloch waves from in-phase precessions within the unit cell, and one band consisting of Bloch waves from the out-of-phase precessions within the unit cells.

To illustrate this idea, in Fig. 6(a) we show the envelope functions of the Bloch waves comprising each band. The applied field is again $h=0.05$. The five lower-frequency envelopes (6–10) are in-phase oscillations between the magnetizations of neighboring films as shown in Fig. 5(a). These waves are analogous to the acoustic elastic waves on a diatomic chain. The five high-frequency envelopes (1–5) are out-of-phase oscillations between the magnetizations of neighboring films as shown in Fig. 5(b). These waves are analogous to the optic elastic waves of a diatomic chain. Thus, the ten modes can be viewed as one band of five acoustic modes and one band of five optic modes.

The mode profiles suggest that the mode amplitudes are sinusoidal functions of position within the multilayer. If L is the total length of the multilayer, then the modes appear to have a wavelength in the multilayer axis direction given by $mL/2$ where m is an integer. We will call this wavelength λ_p:

$$\lambda_p=mL/2\ . \tag{20}$$

The spin-wave modes then fall into two classes: The five

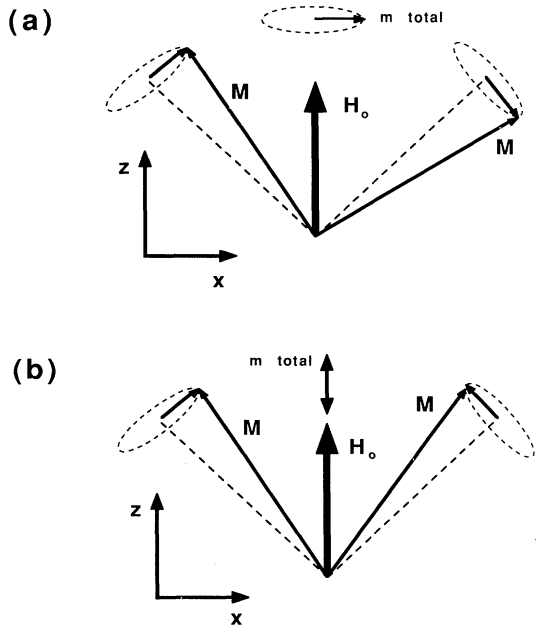

FIG. 5. Precession in a unit cell. The relative motion of the magnetization in a unit cell of a canted superlattice are shown. In phase precession is sketched in (a). The net fluctuations in a unit cell for this case are in the xy plane and are measured by s_{tran} defined by Eq. (18). Out-of-phase precession is sketched in (b). The net fluctuations in a unit cell for this case are in the z direction and are measured by s_{long} defined by Eq. (19).

lowest-frequency modes (acoustic modes) have m running from 0 to 4 with increasing frequency and the five highest-frequency modes (optic modes) have m running from 5 to 1 with increasing frequency.

The acoustic and optic modes differ in a very important way. To understand this, consider the net magnetic fluctuation in a unit cell for each type of mode. It is clear from Fig. 5(a) that the net fluctuating magnetic moment must be mostly in the plane transverse to the applied magnetic field since the longitudinal fluctuations in the field direction will almost cancel across a unit cell. Similarly, from Fig. 5(b) it can be seen that the net transverse fluctuations should cancel across a unit cell while the longitudinal fluctuations add. Thus, the acoustic-type modes represent fluctuations transverse to the applied field and the optic-type modes represent fluctuations in the field direction.

This can be seen in Fig. 6(b) where the amplitude s_{rz} is shown as a function of position across the multilayer for each of the ten modes. The amplitude appears sinusoidal with a period that decreases with increasing mode frequency. s_{rz} oscillates rapidly for the five lowest-frequency modes and the average s_{rz} for the entire multilayer is nearly zero in each case. The five high-frequency modes belong to the optic band, and the average s_{rz} of these modes can be large, especially for mode 1.

These observations are important from the point of view of light scattering from spin waves. This is because the polarization of the incident light in a light scattering experiment will determine which band of spin waves produce the largest scattering cross section. A more complete discussion of this can be found in Ref. 16. In brief, scattering from the acoustic-type modes is strongest if the incident light is polarized in the field direction, since this polarization produces the strongest coupling to the transverse fluctuations. Scattering from the optic-type modes depends on the coupling of the incident light to the longitudinal fluctuations. This is strongest for light polarized

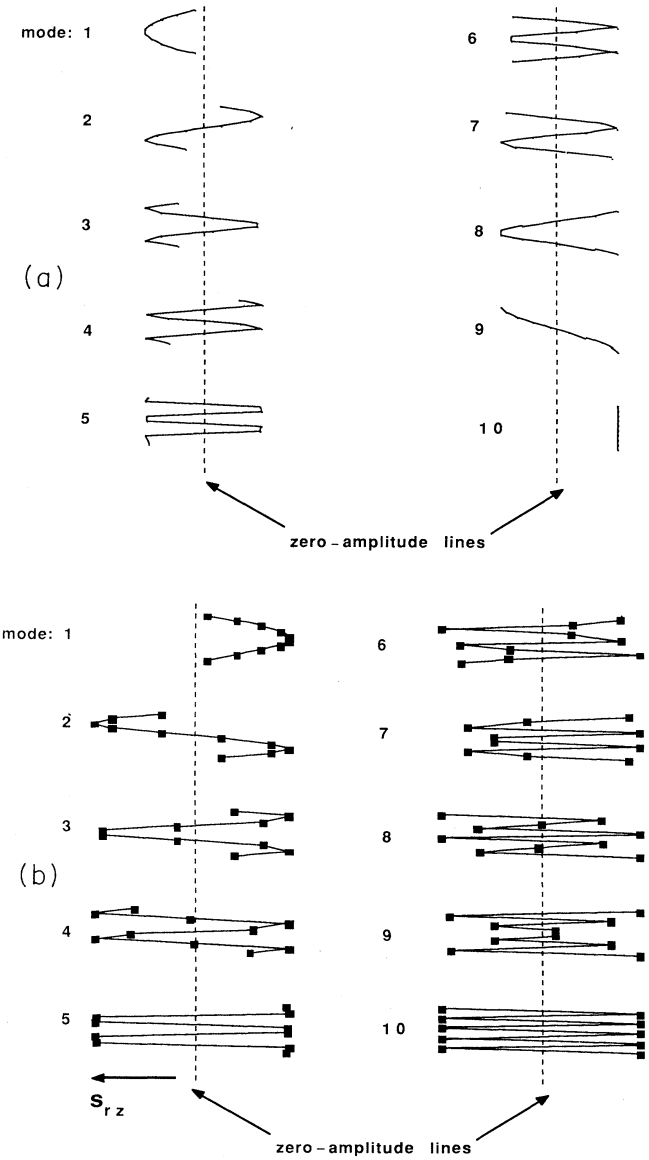

FIG. 6. Bloch wave amplitudes. Modes 1–5 of Fig. 3 are spin waves consisting of coupled out-of-phase precessions in each unit cell. Modes 6–10 of Fig. 3 are spin waves consisting of coupled in-phase precessions in each unit cell. The corresponding Bloch wave amplitudes for both sets of waves are shown in (a). In (b) the amplitude s_z is shown for each of the ten modes from Fig. 3. Note that the net amplitude in the z direction for the entire multilayer is very small for modes 6–10.

in a plane perpendicular to the field direction.

The perpendicular wavelength λ_p of a mode is also important for light scattering from spin waves. The incident electromagnetic field in a light scattering experiment penetrates roughly 100 Å into the multilayer. The largest scattering cross section occurs when the magnetic fluctuations throughout this penetration depth are coherent; i.e., when the amplitude of the spin-wave oscillates slowly as a function of position in the multilayer. The net coupling to an incident electromagnetic field will average to zero if the amplitude of the spin-wave oscillates rapidly over the first 100 Å of the multilayer. This implies that modes with large λ_p will contribute most strongly to the scattering cross section. Thus, mode 10 will provide the largest scattering cross section from the acoustic band. The largest scattering cross section from the optic band will be due to mode 1 because scattering from these modes depend on the longitudinal magnetic fluctuations.

We now discuss the validity of effective-medium theory in light of the above microscopic theory. As discussed in the Introduction, effective-medium theory is valid only for long-wavelength excitations. Furthermore, effective-medium theory does not completely include exchange contributions in the spin-wave energy. We cannot therefore expect that modes with small λ_p will be correctly described by effective-medium theory. The only modes that effective-medium theory can describe are, in fact, modes 1 and 10 of Fig. 3. These are the longest λ_p modes from each band.

A comparison between the two theories is shown in Fig. 7 where the results of an effective-medium calculation for the frequencies of spin waves of a uniformly canted multilayer are plotted as functions of applied field. The effective-medium calculation is for a superlattice of the same net thickness as the earlier microscopic calculations and is shown here by the dark solid lines superimposed on the discrete model calculation of Fig. 3. The frequency of the effective-medium mode which begins at zero frequency for $h=0$ matches that of mode 10 of Fig. 3. The frequency of the effective-medium mode which goes to zero at $h=1.0$ matches that of mode 1. These are the only two modes correctly described by effective medium theory.

As a point of interest, a very simple argument can be used to predict the frequencies of these two modes without using the full apparatus of effective-medium theory. The essential feature is that both of these modes are long-wavelength excitations. One represents a long-wavelength Bloch wave with in-phase precession of the magnetization as in Fig. 6(a). This mode depends on the net magnetization of the structure rather than the magnetization of the individual films. Thus, the frequency of this mode depends on $M_s\cos(\alpha)$. The limiting cases for the frequencies for a thick superlattice structure and a thin superlattice structure are given by and for propagation perpendicular to the magnetic field:

$$\Omega_s = H_0 + 2\pi M_s \cos\alpha \ , \tag{21}$$

$$\Omega_b = \sqrt{H_0(H_0 + 4\pi M_s \cos\alpha)} \ . \tag{22}$$

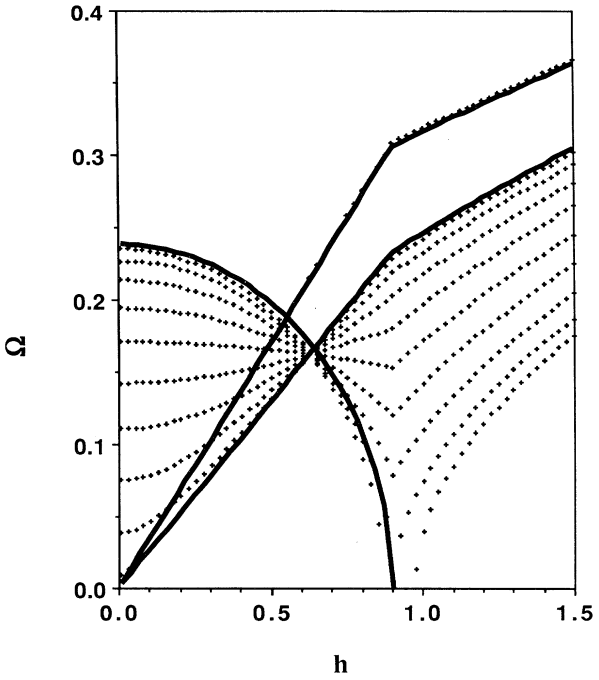

FIG. 7. Effective-medium theory. Results from effective-medium theory are shown superimposed on the results from microscopic theory (Fig. 3). The solid lines are the frequencies of modes predicted by effective-medium theory. The dots are modes predicted by microscopic theory. Note the good agreement between the two theories for modes 1 and 10.

The thick structure result, Eq. (21), is the same as the Damon-Eshbach surface mode in a semi-infinite ferromagnet but where M_s has been replaced by $M_s\cos\alpha$. In the thin structure result the frequency Ω_b of this mode is the same as the uniform ferromagnetic resonance mode again with M_s replaced by $M_s\cos\alpha$.

In contrast, the out-of-phase mode depends on $\sin\alpha$. In the limiting case that the superlattice structure is very thin one finds

$$\Omega_0 = \sqrt{[2(J_i/g\mu_B)](4\pi M_s)}\sin\alpha \ . \tag{23}$$

Note that this equation has the form $\Omega=(2H_eH_a)^{1/2}$ in the limit $\alpha=\pi/2$, an equation familiar from antiferromagnetic resonance theory. A complete discussion of this can be found in Refs. 14 and 16.

We will see in the next section that spin-wave modes in a finite structure with the correct stable ground state cannot be classified as either acoustic or optic in the sense used here. Furthermore, there will be a strong mixing of modes for many values of h that results in all modes having large transverse together with large longitudinal amplitudes. Especially important is that for many h values small λ_p modes will mix with the large λ_p modes. The consequence is that effective-medium theory does not always work if the multilayer is finite.

IV. FINITE-SIZE EFFECTS: THE INFLUENCE OF THE NONUNIFORM GROUND STATE

In a finite system the ground state will not show a uniform canting angle as discussed previously. This nonuniform ground state results in a nonhomogeneous distribution of internal fields which can significantly change the spin excitations in the system.

Spin-wave frequencies are shown in Fig. 8 as functions of applied field for the ground states shown in Figs. 2(b) and 2(c). Propagation is again perpendicular to the field. At small fields, the ground state is similar to that of Fig. 2(b) and at fields near $h=1.0$ the ground state is similar to that of Fig. 2(c). For $h>1$, all the spins are aligned in the direction of the field. The main difference between the spin-wave frequencies in the nonuniform ground state and those in the uniform ground state is that there is a great deal of mode mixing. This is clearly seen in Fig. 8 for h near 0.5 where the Damon-Eshbach mode passes through the bands of bulk modes. The reason for this is that the symmetry of the structure has been significantly lowered. For example, it is no longer possible to define a small unit cell for a ground-state configuration. Here the entire structure is the unit cell. As a result, modes which were orthogonal to one another in the uniform structure are now mixed and mode repulsion is observed. Note that with the correct ground state there is a mode softening at $h=1$ where the magnetization changes from perfectly aligned to canted.

The nonuniform ground states occurs because the multilayers are finite and the outermost films therefore experience a reduced interlayer exchange coupling than films within the multilayer. One might then expect some of the spin waves to be strongly localized to the outermost layers due to the perturbing effects of the outermost surfaces. This is, in fact, the case as seen in Fig. 9 where s_{tran} is shown for $h=0.4$. Although for this value of h the deviations of the canting angles α_n from α given by Eq. (1) are relatively small, the effects on mode mixing are very large. Several of the modes are indeed strongly localized to the outermost films of the multilayer. Also note the lack of symmetry of the mode amplitudes with respect to the midplane of the multilayer.

As mentioned at the end of Sec. III, effective-medium theory can correctly predict the frequencies of two modes if the magnetization is in the uniform ground state of Fig. 2(a). Comparison of Figs. 7 and 8 show, however, that a straightforward application of effective-medium theory does not describe the spin waves properly when the magnetization is in the stable ground states shown in Figs. 2(b) or 2(c). In particular, the mode mixing is not seen in effective-medium theory.

Since perturbing effects of the outermost surfaces will decrease as the number of layers in the multilayer is increased, effective-medium theory should provide a better approximation for very large multilayers. Nevertheless, as shown in Ref. 8, nonuniform canting will occur throughout the entire multilayer for values of h near 0 or 1 regardless of the number of layers. A better description could probably be obtained if effective-medium theory

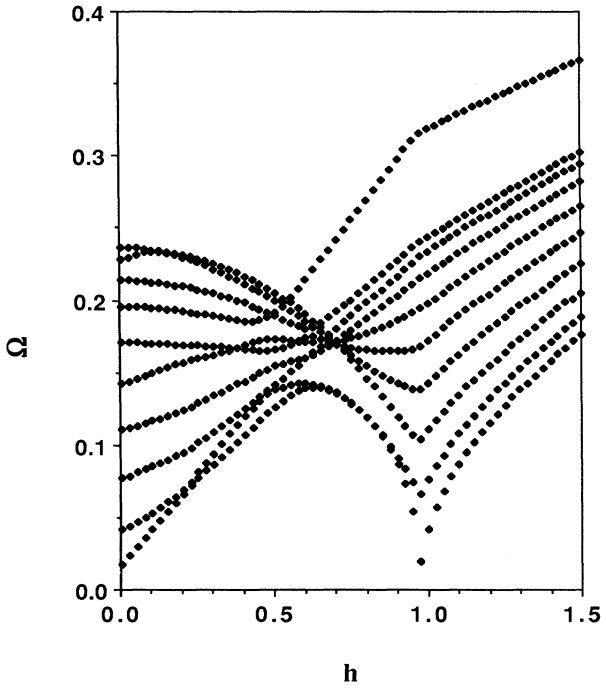

FIG. 8. Finite-size effects. The correct ground-state spin configurations are used in the microscopic calculation of spin-wave energies shown here. The frequencies are shown as functions of applied field for a ten-film multilayer. The ground-state spin configurations resemble those shown in Figs. 2(b) and 2(c) for $h<1$. The spins are parallel in the field direction for $h>1$. Note the strong mixing of modes for $h<1$.

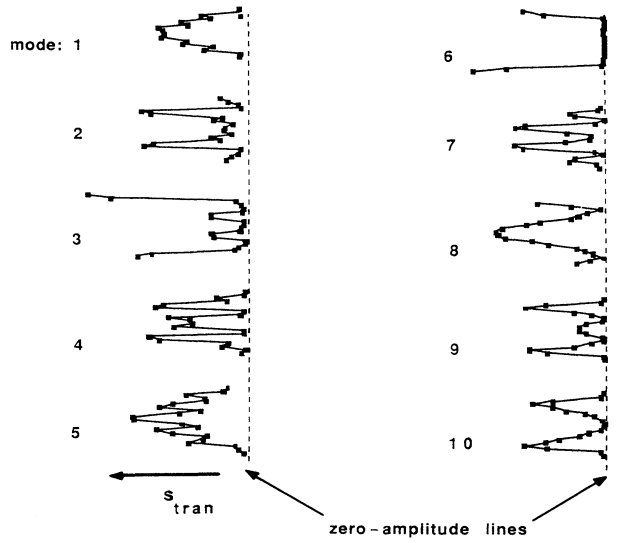

FIG. 9. Localization of modes due to finite size. s_{tran} is shown at $h=0.4$ for the modes of Fig. 8. The finite-size effects are due to the reduced exchange coupling experienced by the outermost films of the multilayer. This leads to a strong mixing of modes and the localization of several mode amplitudes to the outermost films of the multilayer.

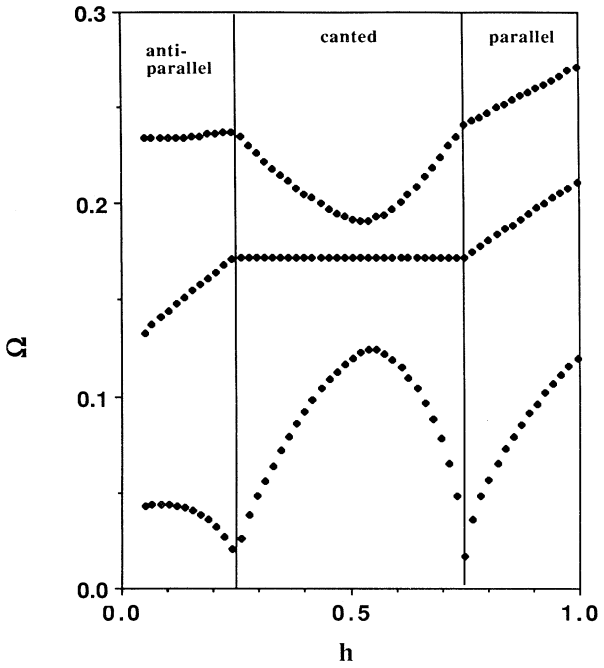

FIG. 10. Spin-wave modes of a trilayer. An antiferromagnetically coupled multilayer with an odd number of magnetic films has a net magnetization that hinders spin canting for small applied field strengths. Here spin-wave frequencies are shown for a three-film structure and are shown as functions of applied field. The spins from different films are antiparallel for $h<0.25$, canted for $0.25<h<0.75$, and parallel for $h>0.75$.

were extended so as to consider local variations in the susceptibility produced by variations in the ground state.

So far we have only considered multilayers consisting of an even number of magnetic films. Another kind of behavior is possible when the number of magnetic layers is odd. An odd number of layers means that the multilayer will always have a net magnetic moment even when the films are aligned antiparallel in zero applied field. The behavior at low fields is then dominated by the Zeeman energy of interaction with the external field: The magnetizations remain antiparallel such that the net magnetization is in the direction of the field. The structure remains aligned like this until the applied field becomes large enough to overcome the cost in exchange energy needed to rotate all the magnetizations partially into the field direction.

The spin-wave energies for an antiferromagnetically coupled trilayer are shown in Fig. 10 as functions of applied field. The magnetizations are antiparallel for h less than 0.25. Every magnetization is canted away from the direction of the field for h between 0.25 and 0.75. For $h>0.75$ the magnetizations are parallel and in the field direction. Note that the frequency of the middle spin-wave mode is nearly independent of h in the canted angle region.

V. PHASE TRANSITIONS IN ANTIFERROMAGNETIC COUPLED MULTILAYERS WITH PERPENDICULAR ANISOTROPY

We would like to remark on a curious prediction of effective-medium theory noted in Ref. 14. It was found that the inclusion of a perpendicular anisotropy energy of the form

$$E_{\rm ani}=\frac{k_a}{M_s^2}m_y^2 \tag{24}$$

leads to a softening of spin-wave modes in a canted multilayer for unusually small values of the anisotropy constant k_a. Here m_y is the component of the fluctuation magnetic moment in a direction perpendicular the magnetic film planes. This behavior is also found in the microscopic model when the in-plane exchange J is small.

The reason for this behavior comes from the dipolar interaction. The dynamic $q\neq 0$ dipolar interaction reduces the spin-wave energies from the $q=0$ values for propagation directions parallel to the field direction. This arises because a finite q excitation induces a spatially oscillating magnetic surface charge on the magnetic layers. These fields tend to reduce the average demagnetizing fields seen by spins in the film interior. This reduction of the average demagnetization fields increases with increasing q.

We can see an example of this effect in a ferromagnetic film. For a very thin film the dispersion relation is given by

$$\omega_{\rm DE}=\frac{g\mu_B}{h}\sqrt{(H_0[H_0+4\pi M_s(1-\tfrac{1}{2}qd)]}\ , \tag{25}$$

where d is the thickness of the film. The reduction in frequency comes from terms in the spin-wave energies of the form

$$4\pi M_s(1-\tfrac{1}{2}qd)\ . \tag{26}$$

These terms ultimately come from the yy component of the $\vec{g}$ tensors [Eqs. (14) and (15)] and appear in this form for $\alpha=0$. qd is small in this approximation so this contribution to the spin-wave energy is always positive.

The situation is more complicated in a multilayer with antiferromagnetic coupling between films. In particular, we consider the case where the external field is small enough so that there is spin canting and $\alpha\neq 0$. As an explicit example, one can show that the frequency of the Damon-Eshbach mode propagating in the field direction on an antiferromagnetically coupled bilayer system is given by[17]

$$\omega_{\rm DE}=\frac{g\mu_B}{\hbar}\{\sqrt{\Omega_b^2+(1-e^{-qs})[4\pi M_s-2(J_i/M_s)\sin^2\alpha]\sin^2\alpha-2\pi H_0M_sqd[\cos^2\alpha+(1+\sin^2\alpha)e^{-qs}]}$$
$$-2\pi M_sqde^{-qs}\sin\alpha\}\ . \tag{27}$$

The thicknesses of the nonmagnetic layer is $s = N_s a$ and Ω_b is the ferromagnetic resonance field for the canted structure given by Eq. (22).

We see that the energy is again reduced by the $M_s qd$ terms, but in a way that depends on the canting angle. Most importantly, the energy is also reduced by the antiferromagnetic exchange coupling J_i.

When a perpendicular anisotropy is present, the $4\pi M_s$ terms in Eq. (27) are replaced by

$$4\pi M_s - 2\frac{k_a}{M_s} . \tag{28}$$

From static energy considerations (a comparison of the energy for the uniformly in-plane magnetized state versus that for the uniformly out-of-plane magnetized state), one can show that when $k_a > 2\pi M_s{}^2$, the magnetization will orient out the film plane in zero applied field. From the forms of Eqs. (27) and (28), one can see that the anisotropy, interlayer exchange, and $M_s qd$ fields act together to reduce the net demagnetization energy $4\pi M_s$. This can, in fact, lead to a softening of modes for values of k_a significantly less than $2\pi M_s{}^2$.

An anisotropy-induced mode softening is shown in Fig. 11 where the two lowest spin-wave frequencies for a canted bilayer structure are shown as functions of $h_a = 2k_a(M_s)$. The parameters for this systems are $qa = 0.006$, $N = 10$, $N_s = 5$, $H_0 = 0.5$ kG, and propagation

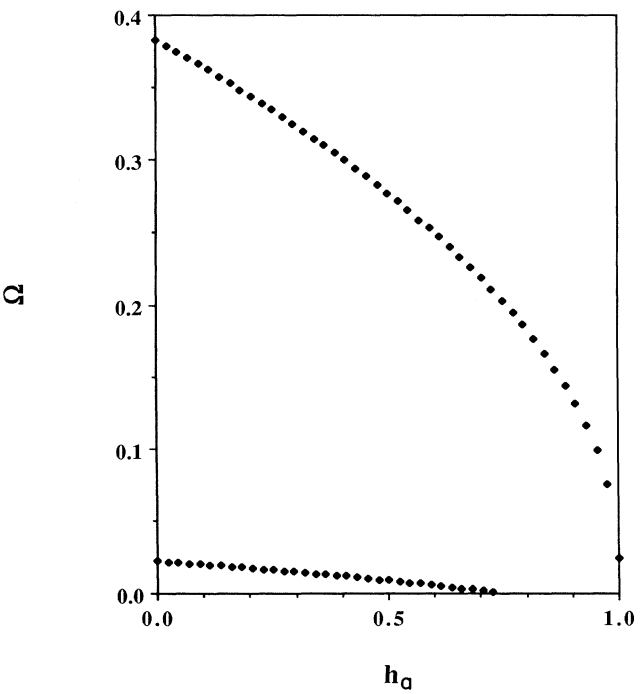

FIG. 11. Instability due to out-of-plane anisotropy. Spin-wave frequencies for a bilayer system are shown as functions of an out-of-plane anisotropy field h_a. The applied field is 0.5 kG so that α is 60°. In plane magnetization for a single thin film becomes unstable for $h_a = 1$. Here, the dynamic demagnetization field and antiferromagnetic exchange interaction lead to a softening of one spin-wave mode for an anisotropy field significantly less than 1.

is in the field direction ($\phi = 0$). The in-plane exchange constant is zero. The higher-frequency mode goes soft at the k_a value where the magnetization would begin tilting out of the film plane in this applied field, but the lower-frequency mode goes soft at a much smaller k_a value as described above. As the in-plane exchange constant is increased from zero, the lower frequency mode softens at larger k_a values. The two modes soften at approximately the same k_a value for realistic exchange constant magnitudes.

We interpret this softening as an indication that a uniform magnetization within the magnetic films is no longer energetically favorable and that some type of domainlike structure would be the stable ground state. In particular, it may be possible to reduce the magnetostatic and antiferromagnetic energies by forming a magnetic ground state wherein the magnetizations of the two films try to align antiparallel in the out-of-plane direction. This state would involve a rotation of the spin directions over large distances in order to minimize the cost of intralayer exchange energy. Although this may be an uninteresting effect for perfect films with large ferromagnetic exchange constants, we note that this instability may occur in systems composed of antiferromagnetically coupled ultrathin films with imperfections. This may also occur in certain easy plane antiferromagnets where a weak in-plane ferromagnet coupling exists.

VI. NONRECIPROCITY

One of the well-known features of spin waves with dipolar contributions is that they can be nonreciprocal in the sense that a reversal of the wave vector does not necessarily lead to a wave with the same frequency, i.e., $\omega(\mathbf{q}) \neq \omega(-\mathbf{q})$. This is particularly dramatic for a surface spin wave on a semi-infinite ferromagnet where a surface wave exists for some propagation directions but does not exist when the propagation direction is reversed. In this section we will show that a great deal can be learned about the dependence of spin-wave energies in canted structures on propagation direction through simple symmetry considerations.

The basic idea here is that if we can perform an operation (reflections, rotations, or combinations of these) on the system and change the wave vector from $\mathbf{q}$ to $-\mathbf{q}$ but leave the magnetic system and the applied field unchanged, then we must have reciprocal behavior in the frequency. In this case we must have $\omega(\mathbf{q}) = \omega(-\mathbf{q})$ because the energy of the excitation cannot be changed by a symmetry operation. If we cannot perform such an operation then nonreciprocal behavior is allowed (but not required).

In particular, we will determine if the frequency of a spin wave traveling in a canted structure with wave vector $\mathbf{q} = (q_x, q_z)$ is equivalent to that of a spin wave traveling with wave vector where either q_x has been reversed or q_z has been reversed or both q_x and q_z are reversed. To illustrate how these symmetry arguments work, we first consider the case of a spin wave traveling perpendicular to the field in a multilayer with an even number of magnetic layers.

First, we define a geometry as shown in Fig. 12(a). The applied field is directed into the page in the $+z$ direction. The magnetization of each film is assumed to be canted away from the direction of the applied field as in the ground state of Fig. 2(b). In Fig. 12, we represent the magnetizations in each film by a component in the field direction, M_z, and a component perpendicular to the field, M_x. The wave vector $\mathbf{q}$ is also shown perpendicular to the magnetization in the $+x$ direction. The ground-state configuration of the magnetization is assumed to be symmetric with respect to the midplane of the multilayer. A simple rotation of 180° about the z axis takes the structure and the field into themselves but reverses the direction of $\mathbf{q}$. Thus, the propagation frequency is reciprocal; i.e. $\omega(\mathbf{q})=\omega(-\mathbf{q})$.

Suppose instead that $\mathbf{q}$ is directed along the $+z$ direction. The change q_z to $-q_z$ we need to reflect in the plane of the paper. The results of this reflection are illustrated in Fig. 12(b). The external field H_0 and the M_z components are left unchanged but M_x is reversed. One could try to get back to the original structure by reflecting about the midplane of the structure. Such an operation reverses the positions of the upper and lower films and then reverses both M_x and M_z in each film as well as reversing the applied field. But the resulting structure is not the same as the original structure. In fact, we have found no operation which takes q_z to $-q_z$ and leaves the structure unchanged when q has a component along the z axis. Thus nonreciprocal behavior is allowed for any direction of propagation which has a component of the wave vector parallel to the applied field.

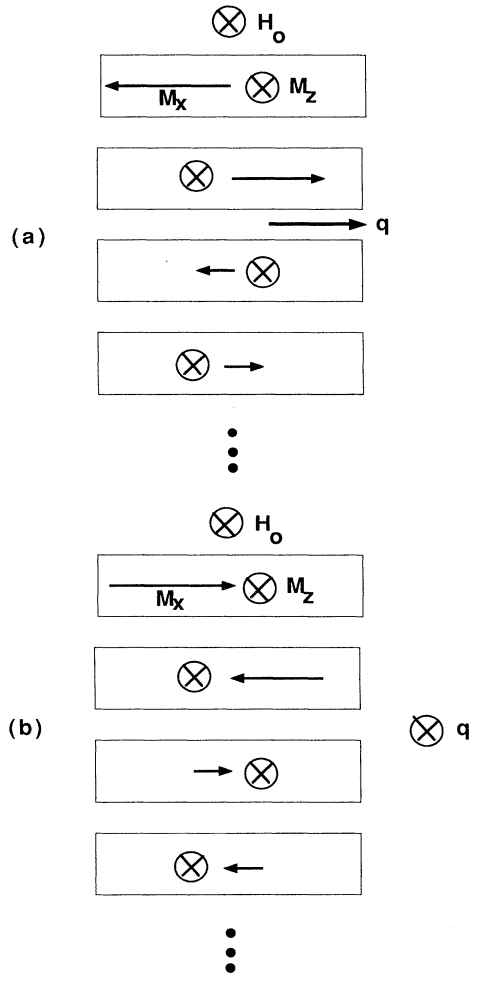

FIG. 12. Symmetry operations. The initial spin configuration for a multilayer is defined in (a). The applied field is directed into the page and a wave vector $\mathbf{q}$ is perpendicular to the field. In (b) the initial wave vector $\mathbf{q}$ was directed opposite the field and a reflection through the midplane of the page has been made.

In addition to examining nonreciprocal behavior where the entire wave vector is reversed, these symmetry arguments can be used to look at situations where only one component of the wave vector is reversed. The general results for the structure with an even number of layers are found in a similar manner and are summarized below.

(1) Propagation symmetries for an even number of layers:

$$\omega(q_x,q_z)=\omega(-q_x,q_z)\ , \tag{29}$$

$$\omega(q_x,q_z)\neq\omega(q_x,-q_z)\ , \tag{30}$$

$$\omega(q_x,q_z)\neq\omega(-q_x,-q_z)\ . \tag{31}$$

This nonreciprocal behavior can be seen in Fig. 13(a) where the spin-wave frequencies are shown as functions of propagation direction angle ϕ. The field h is 0.53 and there are ten magnetic films in the multilayer. The ground state for this field is similar to that shown in Fig. 2(a). The lowest-energy modes show a strong nonreciprocity in frequency between propagation parallel to the applied field ($\phi=0°$) and propagation antiparallel to the applied field ($\phi=180°$). In fact, the frequencies are only reciprocal for propagation perpendicular to the field, $\phi=90°$ and 270°. From the symmetry results presented above we see that the graph of Ω versus ϕ should be symmetric about $\phi=0°$ and 180°, and this is confirmed in Fig. 13.

The magnitude of the nonreciprocity depends on the canting angle ground-state configuration. This is shown in Fig. 13(b) where the spin-wave frequencies are again shown as functions of ϕ with $h=0.8$. The average canting angle is now much smaller than in Fig. 13(a) and the ground state resembles that of Fig. 2(b). Nonreciprocity for all propagation directions other than 90° and −90° is still visible, but the magnitude is less than in Fig. 13(a).

The allowed symmetry operations for multilayers with an odd number of magnetic layers are different than for multilayers with an even number of magnetic layers. For the odd number case, arguments similar to those above show that the spin-wave frequencies are always reciprocal; i.e., $\omega(q)=\omega(-q)$ regardless of the direction of q. However, reversal of a single component of the wave vector does not always lead to a mode with the same frequency. The general results are given below.

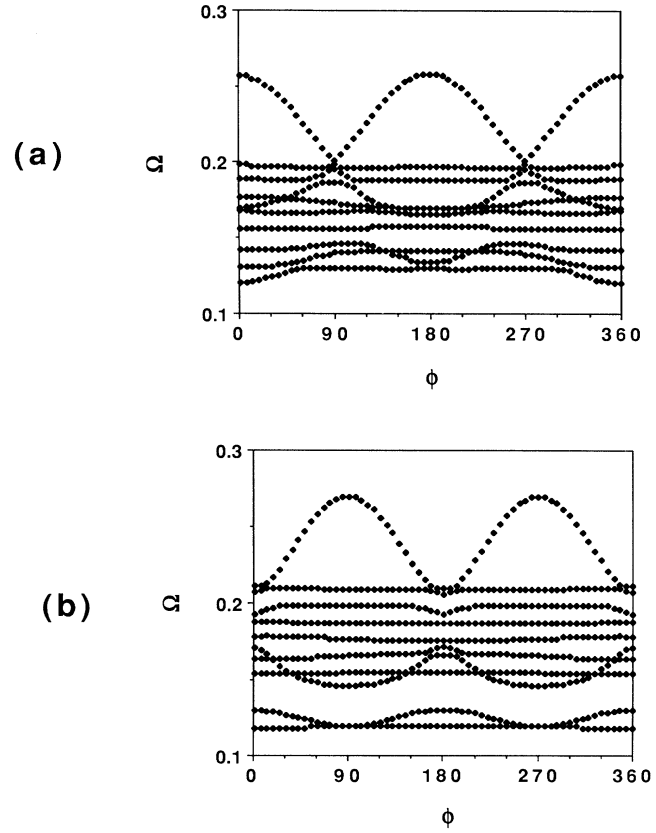

FIG. 13. Dependence on propagation direction for an even number of films. Spin-wave frequencies are shown as functions of propagation angle ϕ. There are ten magnetic films with the same parameters as in Fig. 8. The applied field h is 0.53 in (a). Note the large differences in frequencies between propagation parallel to the field ($\phi=0°$) and antiparallel to the field ($\phi=180°$). The applied field h is 0.8 in (b). Here the canting angles are smaller and the nonreciprocities are less pronounced than in (a).

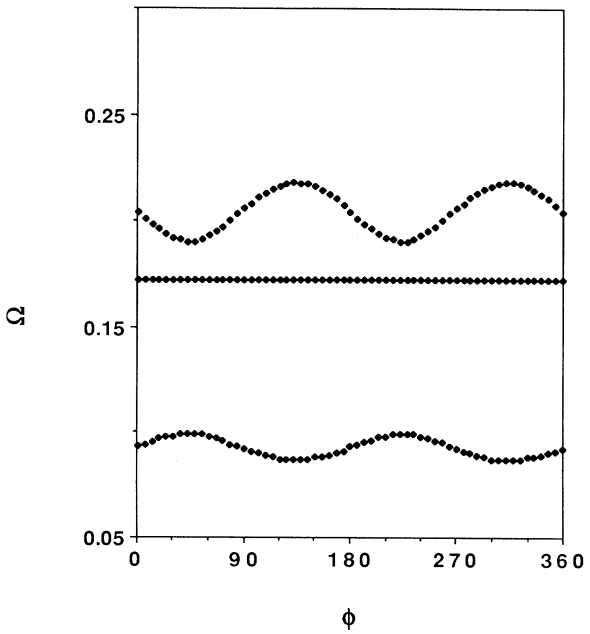

FIG. 14. Dependence on propagation direction for an odd number of films. Spin-wave modes for the trilayer structure (see Fig. 11) are shown as functions of ϕ with $h=0.4$. Propagation is reciprocal [$\omega(q)=\omega(-q)$] for all directions. Note, however, that $\omega(q_x,q_z)\neq\omega(-q_x,q_z)$.

(2) Propagation symmetries for an odd number of layers:

$$\omega(q_x,q_z)\neq\omega(-q_x,q_z)\ , \tag{32}$$

$$\omega(q_x,q_z)\neq\omega(q_x,-q_z)\ , \tag{33}$$

$$\omega(q_x,q_z)=\omega(-q_x,-q_z)\ . \tag{34}$$

These relationships mean that Ω versus ϕ is not symmetric about $\phi=180°$ and also not symmetric about $\phi=90°$ or 270°. However, the spin-wave frequencies are periodic with period 180°. An example is presented in Fig. 14 where the spin-wave frequencies for the trilayer structure of Fig. 11 are shown as functions of ϕ. The applied field h is 0.4. We see the frequencies are always reciprocal with respect to propagation direction, i.e., a change of 180° in ϕ gives the same frequency.

The origin of the nonreciprocity can be understood in terms of the development presented in this paper. Examination of $\vec{g}(q;n-n')$ in Eq. (14) shows that the dipolar interaction introduces a q-dependent "anisotropy" field into the spin-wave energies. As an example, consider the Damon-Eshbach mode on a simple ferromagnet. This q-dependent "anisotropy" leads to a large difference in energy between propagation perpendicular and propagation parallel to the field direction. The symmetry axes for this q-dependent "anisotropy" are governed by the direction of propagation and the ground-state configuration of the magnetization.

Finally, we note that a straightforward application of effective-medium theory is by its nature unable to correctly give the nonreciprocity. For example, the effective-medium system cannot distinguish between systems with odd numbers of layers and even numbers of layers.

VII. SUMMARY

The properties of spin waves on antiferromagnetically coupled magnetic multilayers have been examined assuming the correct stable ground-state orientations of the magnetization. Spin waves on infinite antiferromagnetically coupled superlattices can be classified as either acoustic or optic modes in analogy to elastic excitations. Acoustic modes correspond to magnetic fluctuations transverse to the applied field and optic modes correspond to magnetic fluctuations in the field direction. These distinctions are particularly important for light scattering experiments, since the coupling of incident light is strongly dependent on geometry.

In finite structures the stable ground states are sometimes quite complex configurations due to surface effects. Spin-wave modes on finite antiferromagnetically coupled multilayers have mixed optic and acoustic mode proper-

ties due to the nonuniform canting of the stable ground states. Also, in some cases mode amplitudes will be strongly localized to an outermost film of the multilayer.

Effective medium theory was examined by comparison to a microscopic discrete model. It was found that effective-medium theory can only describe two modes properly: The Damon-Eshbach mode (the longest-wavelength acoustic mode) and the longest-wavelength optic mode. Since effective-medium theory does not properly take interlayer exchange interactions into account, it is unable to describe any other shorter-wavelength mode. Furthermore, effective medium does not accurately predict the frequencies of these two modes when finite-size effects are considered. Effective-medium theory is only approximately valid for these two modes on very large multilayers and for a limited range of external applied field strengths.

The energy of the spin-wave modes are strongly influenced by dipolar interactions at long wavelengths. The dipolar interactions act as a kind of anisotropy and depend on the symmetry of the magnetic system. Symmetry arguments show that spin-wave propagation on canted structures may always be nonreciprocal unless propagation is perpendicular to the applied field or the number of magnetic layers in the multilayer is odd.

Finally, it was noted that the antiferromagnetic interlayer exchange interaction together with a relatively small perpendicular anisotropy may destabilize a uniform ferromagnetic ordering in the films. This effect should be small for perfect ferromagnetic films with strong intralayer exchange coupling, but may be observable for multilayers, imperfect films, and some easy plane antiferromagnets.

ACKNOWLEDGMENTS

The work of R. L. S. and R. E. C. was supported by the US Army Research Office under Grant No. DAAL0391-G-0229. F. C. N. thanks G. Güntherodt of the RWTH Aachen for support.

APPENDIX

The dipole sums of Eq. (3) can be put in rapidly convergent forms using the method of Ref. 15. The sums differ depending on whether the sources are in the same plane, where $n=n'$, or if the sources are in other planes so that $n\neq n'$. For our geometry, the $n\neq n'$ sums are

$$g_{xx}(\mathbf{q};n-n')=\frac{4\pi}{a^3}\sum_{k=-\infty}^{\infty}\sum_{m=-\infty}^{\infty}\frac{\beta_m^2}{\sqrt{\beta_k^2+\beta_m^2}}e^{-2|n-n'|\sqrt{\beta_k^2+\beta_m^2}}, \tag{A1}$$

$$g_{yy}(\mathbf{q};n-n')=-\frac{4\pi}{a^3}\sum_{k=-\infty}^{\infty}\sum_{m=-\infty}^{\infty}\sqrt{\beta_k^2+\beta_m^2}\,e^{-2|n-n'|\sqrt{\beta_k^2+\beta_m^2}}, \tag{A2}$$

$$g_{zz}(\mathbf{q};n-n')=\frac{4\pi}{a^3}\sum_{k=-\infty}^{\infty}\sum_{m=-\infty}^{\infty}\frac{\beta_k^2}{\sqrt{\beta_k^2+\beta_m^2}}e^{-2|n-n'|\sqrt{\beta_k^2+\beta_m^2}}, \tag{A3}$$

$$g_{xy}(\mathbf{q};n-n')=g_{yx}(\mathbf{q};n-n')=-\frac{4\pi i}{a^3}\mathrm{sgn}(n-n')\sum_{k=-\infty}^{\infty}\sum_{m=-\infty}^{\infty}\beta_m e^{-2|n-n'|\sqrt{\beta_n^2+\beta_m^2}}, \tag{A4}$$

$$g_{yz}(\mathbf{q};n-n')=g_{zy}(\mathbf{q};n-n')=-\frac{4\pi i}{a^3}\mathrm{sgn}(n-n')\sum_{k=-\infty}^{\infty}\sum_{m=-\infty}^{\infty}\beta_k e^{-2|n-n'|\sqrt{\beta_k^2+\beta_m^2}}, \tag{A5}$$

$$g_{xz}(\mathbf{q};n-n')=g_{zx}(\mathbf{q};n-n')=\frac{4\pi}{a^3}\sum_{k=-\infty}^{\infty}\sum_{m=-\infty}^{\infty}\frac{\beta_k\beta_m}{\sqrt{\beta_k^2+\beta_m^2}}e^{-2|n-n'|\sqrt{\beta_k^2+\beta_m^2}}, \tag{A6}$$

where

$$\beta_k=\tfrac{1}{2}qa\sin\phi+k\pi, \tag{A7}$$

$$\beta_m=\tfrac{1}{2}qa\cos\phi+m\pi. \tag{A8}$$

The $n=n'$ sums are

$$g_{xx}(\mathbf{q};0)=\frac{16\pi}{3a^3}\sum_{k=1}^{\infty}\sum_{m=-\infty}^{\infty}\begin{Bmatrix}\cos(kqa\cos\phi)(\frac{1}{2}qa\sin\phi+m\pi)^2K_2(2k|\frac{1}{2}qa\sin\phi+m\pi|)\\ -2\cos(kqa\sin\phi)(\frac{1}{2}qa\cos\phi+m\pi)^2K_2(2k|\frac{1}{2}qa\cos\phi+m\pi|)\end{Bmatrix}, \tag{A9}$$

$$g_{yy}(\mathbf{q};0)=\frac{16\pi}{3a^3}\sum_{k=1}^{\infty}\sum_{m=-\infty}^{\infty}\begin{Bmatrix}\cos(kqa\cos\phi)(\frac{1}{2}qa\sin\phi+m\pi)^2K_2(2k|\frac{1}{2}qa\sin\phi+m\pi|)\\ +\cos(kqa\sin\phi)(\frac{1}{2}qa\cos\phi+m\pi)^2K_2(2k|\frac{1}{2}qa\cos\phi+m\pi|)\end{Bmatrix}, \tag{A10}$$

and

$$g_{zz}(\mathbf{q};0)=\frac{16\pi}{3a^3}\sum_{k=1}^{\infty}\sum_{m=-\infty}^{\infty}\left\{\begin{array}{l}\cos(kqa\,\sin\phi)(\frac{1}{2}qa\,\cos\phi+m\pi)^2K_2(2k|\frac{1}{2}qa\,\cos\phi+m\pi|)\\ -2\cos(kqa\,\cos\phi)(\frac{1}{2}qa\,\sin\phi+m\pi)^2K_2(2k|\frac{1}{2}qa\,\sin\phi+m\pi|)\end{array}\right\}. \tag{A11}$$

In Eqs. (A9)–(A11), K_2 is a modified Bessel function of the second kind.

---

*Currently at 2. Physikalisches Institut, RWTH Aachen, Templergraben 55, 5100 Aachen, Germany.

[1]P. Grünberg, R. Schreiber, Y. Pang, M. B. Brodsky, and H. Sowers, Phys. Rev. Lett. **57**, 2442 (1986).

[2]M. N. Baibich, J. M. Broto, A. Fert. F. Nguyen Van Dau, F. Petroff, P. Etienne, G. Creuzet, A. Friederich, and J. Chazelas, Phys. Rev. Lett. **61**, 2472 (1988).

[3]G. Binasch, P. Grünberg, F. Saurenbach, and W. Zinn, Phys. Rev. B **39**, 4828 (1989).

[4]S. S. P. Parkin, N. More, and K. P. Roche, Phys. Rev. Lett. **64**, 2304 (1990).

[5]R. E. Camley and J. Barnas, Phys. Rev. Lett. **63**, 664 (1989).

[6]P. M. Levy, S. Zhang, and A. Fert, Phys. Rev. Lett. **65**, 1643 (1990).

[7]A. Vedyayev, B. Dieny, and N. Ryzhanova, Europhys. Lett. **19**, 329 (1992).

[8]F. C. Nörtemann, R. L. Stamps, A. S. Carriço, and R. E. Camley, Phys. Rev. B **46**, 10 847 (1992).

[9]A. S. Borovik-Romanov and N. M. Kreines, in *Spin Waves and Magnetic Excitations I,* edited by A. S. Borovik-Romanov and S. K. Sinha (Elsevier, New York, 1988); B. Hillebrands, in *Light Scattering in Solids,* edited by M. Cardona and G. Güntherodt (Springer, Berlin, to be published).

[10]P. Grünberg, in *Light Scattering in Solids V,* edited by M. Cardona and G. Güntherodt (Springer, Berlin, 1989).

[11]N. S. Almeida and D. L. Mills, Phys. Rev. B **38**, 6698 (1988).

[12]N. Raj and D. R. Tilley, Phys. Rev. B **36**, 7003 (1987).

[13]J. Fassbender, F. Nörtemann, R. L. Stamps, R. E. Camley, B. Hillebrands, G. Güntherodt, and S. S. P. Parkin, Phys. Rev. B **46**, 5810 (1992).

[14]F. Nörtemann, R. L. Stamps, R. E. Camley, B. Hillebrands, and G. Güntherodt, Phys. Rev. B **47**, 3225 (1993).

[15]H. Benson and D. L. Mills, Phys. Rev. **178**, 839 (1969); R. P. Erickson and D. L. Mills, Phys. Rev. B **43**, 10 715 (1991); **44**, 11 825 (1991).

[16]R. L. Stamps, R. E. Camley, F. C. Nörtemann, and D. R. Tilley (unpublished).

[17]R. L. Stamps (unpublished).